Thermal Dissociation of Condensed Complexes of Cholesterol and Phospholipid

Arun Radhakrishnan and Harden M. McConnell*

Department of Chemistry, Stanford University, Stanford, California 94305

Received: October 23, 2001; In Final Form: February 25, 2002

Many saturated phospholipids and mixtures of saturated phospholipids have been found to form complexes with cholesterol in monolayers in the liquid state at the air−water interface. However, in these monolayers, one saturated phospholipid, dimyristoylphosphatidylcholine, shows no evidence for complex formation in mixtures with cholesterol (or dihydrocholesterol) at room temperature. Here we report clear evidence for the formation of complexes in these mixtures at 13 °C. At this temperature, the liquid−liquid immiscibility phase diagrams show two upper miscibility critical points with an intervening cusp at a putative stoichiometric composition. Furthermore, the chemical activity of cholesterol shows a large change at this same composition. Neither of these signatures of complex formation is observed at room temperature. The phase diagrams at the two temperatures can be modeled semiquantitatively in terms of the formation of a 3:2 phospholipid/cholesterol complex, with an exothermic heat of formation of 9 kcal/mol of phospholipid. This heat of reaction is comparable to the heat of reaction inferred from scanning calorimetry of bilayers of these mixtures.

Introduction

In early work, it was recognized that monolayer mixtures of a number of saturated phospholipids and cholesterol are nonideal. For example, at a given monolayer pressure, a binary mixture of a phospholipid and cholesterol may have an average molecular area that is significantly less than the sum of the molecular areas of the two components. This nonadditivity of the molecular areas was described as a "condensing effect" of cholesterol.[1] It has also been proposed that cholesterol and phospholipids form complexes.[2,3] More recent models for the properties of these mixtures are summarized in the book by Feingold.[4] In still more recent studies of cholesterol−phospholipid monolayers, this condensing effect has been attributed to the formation of "condensed complexes" of cholesterol and phospholipid. Qualitatively, these complexes are clusters of cholesterol and phospholipid molecules having a specific composition. Quantitatively, these complexes have been characterized thermodynamically in terms of a reversible chemical equilibrium reaction between cholesterol and phospholipid to form a complex.[5] The presence of such complexes in monolayers has been inferred from theoretical modeling of average molecular area measurements, observations of coexisting liquid phases at lower monolayer pressures using epifluorescence microscopy, and cholesterol desorption experiments.[6,7]

Previous work has described a rule-of-thumb correlation, for at least some phospholipid classes, between the formation of condensed complexes in monolayers at room temperature and the chain-melting transition temperatures of the pure phospholipids in bilayers. A number of phospholipids having chain-melting temperatures above room temperature show clear evidence of complex formation at room temperature, whereas phospholipids with melting temperatures below room temperature often show no evidence for condensed complex formation at room temperature.[8] Dimyristoylphosphatidylcholine (DMPC) has a melting temperature of 23 °C in bilayers. Extensive studies of liquid−liquid immiscibility in binary mixtures of cholesterol and DMPC at room temperature have shown no evidence for complex formation. However, the proximity of the DMPC melting temperature to room temperature suggested to us that this phospholipid might form complexes with cholesterol at lower temperatures. In the present work, we report clear evidence for the formation of these complexes in monolayers at 13 °C. Three criteria are used as evidence: (i) liquid−liquid immiscibility phase diagrams, (ii) average molecular areas, and (iii) the rates of cholesterol desorption to β-cyclodextrin.

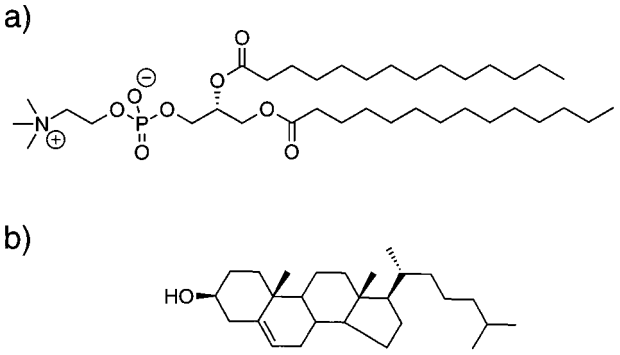

Figure 1. Chemical structures of (a) dimyristoylphosphatidylcholine (DMPC) and (b) cholesterol. Dihydrocholesterol (Dchol) is structurally similar to cholesterol except that the double bond is hydrogenated.

Methods

Phase Diagrams. DMPC was obtained from Avanti Polar Lipids, Alabaster, AL, and cholesterol and dihydrocholesterol (Dchol) were obtained from Sigma, St. Louis, MO (see Figure 1). Texas Red-dihexadecanoylphosphatidylethanolamine (TR-DHPE) was obtained from Molecular Probes, Eugene, OR. These lipids were used without further purification in experiments carried out at room temperature, 23 ± 0.5 °C, and at 13 ± 0.5 °C. Phase diagram measurements were carried out using epifluorescence microscopy and methods described previously.[9,10] Monolayers of DMPC/sterol mixtures were spread from 1 mg/mL chloroform solutions onto the air−water interface of a Teflon trough with a movable barrier to vary the surface

* Corresponding author. E-mail: harden@stanford.edu. Tel: (650) 723-4571. Fax: (650) 725-0259.

10.1021/jp013932d CCC: $22.00
Published on Web 04/11/2002

pressure. The subphase contained distilled water at pH 5.3. Substitution with phosphate-buffered saline made no significant difference in the phase behavior. For many of these mixtures, two-phase coexistence can be visualized at the lower pressures by incorporating 0.2 mol % of the probe TR-DHPE. This dye provides contrast by being preferentially excluded from the sterol-rich phase. Transition pressures are marked by the disappearance of two-phase coexistence during monolayer compression and thus define a phase boundary. Molecular area measurements are obtained by depositing small aliquots of the lipid mixtures until a given surface pressure (20 dyn/cm) is reached.

Desorption Kinetics. The rate of release of cholesterol from the monolayer membrane due to desorption by beta-cyclodextrin (β-CD) is a measure of the chemical activity of cholesterol in the membrane.[7] β-CD was obtained from Sigma, St.Louis, MO. The desorption of cholesterol (or Dchol) to a subphase containing 1 mM or 2 mM β-CD was monitored by the decrease in the monolayer area necessary to maintain a constant surface pressure of 20 dyn/cm. As described earlier,[7] rate constants for cholesterol or Dchol desorption were calculated from the area vs time data in conjunction with the molecular area measurements.

Most of the reported experiments were carried out using Dchol rather than cholesterol so as to minimize artifacts due to air oxidation. We have previously found that using Dchol instead of cholesterol yields slightly lower values of the phase-transition pressures,[11] but the phase behavior of the two sterols is virtually identical otherwise. In the phase diagrams and desorption measurements outlined above, controls were always carried out using cholesterol itself in a chamber flooded with argon gas and with the subphase containing argon-saturated water.

Theoretical Modeling

A mean-field thermodynamic model[6,12,13] was extended to describe the temperature effects observed in this study. As before, we consider a mixture of two liquid components, C (cholesterol or Dchol) and P (phospholipid), that react to form a complex $C_{nq}P_{np}$,

$$nq\mathrm{C} + np\mathrm{P} \overset{K_{eq}}{\rightleftharpoons} \mathrm{C}_{nq}\mathrm{P}_{np} \tag{1}$$

Here q and p are relatively prime stoichiometry integers, and n is an oligomerization parameter reflecting the cooperativity of this reaction.

The free energy for this reactive mixture is

$$G = Nk_{\mathrm{B}}T\sum_i x_i \ln x_i + Nk_{\mathrm{B}}T^0\sum_{i<j} a_{ij}x_i x_j + N\sum_i x_i\mu_i^0 \tag{2}$$

where N is the equilibrium number of molecules in the sample, k_{B} is Boltzmann's constant, and x_i and μ_i^0 are, respectively, the mole fractions and the standard chemical potentials of the three species C, P, and $C_{nq}P_{np}$. The standard chemical potentials are at reference conditions of $T^0 = 296$ K and $\pi^0 = 0$ dyn/cm. Note that T^0 is a constant, not a variable. The a_{ij}'s are energy parameters in units of $k_{\mathrm{B}}T^0$ describing a mean-field repulsion between the molecular pairs. Diagonal (a_{ii}) and higher-order terms are omitted for simplicity. These energy parameters are linear functions of the monolayer surface pressure π:

$$a_{ij} = 2 + a'_{ij}(\pi - \pi_{ij}) \tag{3}$$

Here the π_{ij}'s are the critical pressures of the hypothetical nonreacting binary mixtures of i and j, and the a'_{ij}'s have units of reciprocal surface pressure. Note that surface pressure is defined as the difference between the surface tension of water and that of the monolayer. In our work, we have neglected the 2% change in the surface tension of water between 23 and 13 °C.

The standard chemical potential of the complex, $\mu^0_{C_{nq}P_{np}}$, is related to the reactant standard chemical potentials through the reaction equilibrium constant:

$$\mu^0_{\mathrm{C}_{nq}\mathrm{P}_{np}} = nq\mu^0_{\mathrm{C}} + np\mu^0_{\mathrm{P}} - k_{\mathrm{B}}T\ln K^0_{\mathrm{eq}} \tag{4}$$

The equilibrium constant varies with the surface pressure π and temperature T according to the equation

$$K_{\mathrm{eq}} = K^0_{\mathrm{eq}}\exp\left[-\frac{(\pi-\pi^0)\Delta A}{k_{\mathrm{B}}T} + \frac{\Delta H}{k_{\mathrm{B}}}\left(\frac{1}{T^0}-\frac{1}{T}\right)\right] \tag{5}$$

Here ΔA and ΔH are the area change and heat of reaction corresponding to eq 1. The area change of reaction 1 is defined as $\Delta A = A_{C_{nq}P_{np}} - nqA_{\mathrm{C}} - npA_{\mathrm{P}}$, and the heat of reaction 1 is $\Delta H = np\Delta H_{\mathrm{P}}$, where ΔH_{P} is the heat of reaction per mole of P. K^0_{eq} is the equilibrium constant of reaction 1 at the standard conditions of temperature and pressure defined above.

In comparing different cholesterol−phospholipid complexes, it is useful to introduce a normalized form of the reaction in eq 1:

$$q\mathrm{C} + p\mathrm{P} \overset{\hat{K}_{\mathrm{eq}}}{\rightleftharpoons} \frac{1}{n}\,\mathrm{C}_{nq}\mathrm{P}_{np} \tag{6}$$

This normalized form of the reaction is described by the thermodynamic parameters, $\Delta\hat{A}$, $\Delta\hat{H}$, and $\hat{K}_{\mathrm{eq}}$, where $\Delta\hat{A} = \Delta A/n$, $\Delta\hat{H} = \Delta H/n$, and $\hat{K}_{\mathrm{eq}} = (K_{\mathrm{eq}})^{1/n}$.

In the calculations, the free energy G is minimized with respect to the extent of reaction γ, defined as

$$\gamma = N_{\mathrm{C}_{nq}\mathrm{P}_{np}}/N_0 \tag{7}$$

where N_0 is the number of molecules present if no reaction occurs. The mole fractions x_i are determined by γ and can be written

$$x_{\mathrm{C}} = (x_0 - nq\gamma)\zeta$$
$$x_{\mathrm{P}} = (1 - x_0 - nq\gamma)\zeta$$
$$x_{\mathrm{C}_{nq}\mathrm{P}_{np}} = \gamma\zeta$$
$$\zeta = [1 + (1 - np - nq)\gamma]^{-1} \tag{8}$$

Here x_0 is the mole fraction of C in the sample before reaction.

The free energy can thus be expressed as a function of four variables, $G = G(x_0, \pi, T, \gamma)$, along with a number of parameters ($\hat{K}^0_{\mathrm{eq}}$, $\Delta\hat{A}$, ΔH_{P}, a'_{ij}, π_{ij}, q, p, and n). This free energy is minimized with respect to γ at fixed (x_0, π, T) to find the equilibrium extent of reaction γ_{eq}. The equilibrium compositions are obtained using γ_{eq} and eq 8. The normalized equilibrium extent of reaction is defined as $\gamma_{\mathrm{eq}}/\gamma_{\max}$, where $\gamma_{\max}$ is the maximum possible extent of reaction at the stoichiometric composition of $x_0 = q/(p+q)$. If the free energy of the sample can be reduced by phase separation, a double tangent construction is used to determine the compositions of the two coexisting phases and generate phase diagrams. The chemical activity of C is $\exp[\mu_{\mathrm{C}}/k_{\mathrm{B}}T]$, where the chemical potential μ_{C} is $\partial G/\partial N_{\mathrm{C}}$.

The values of many of the parameters that are used are fixed directly by the experimental data. For example, the value for

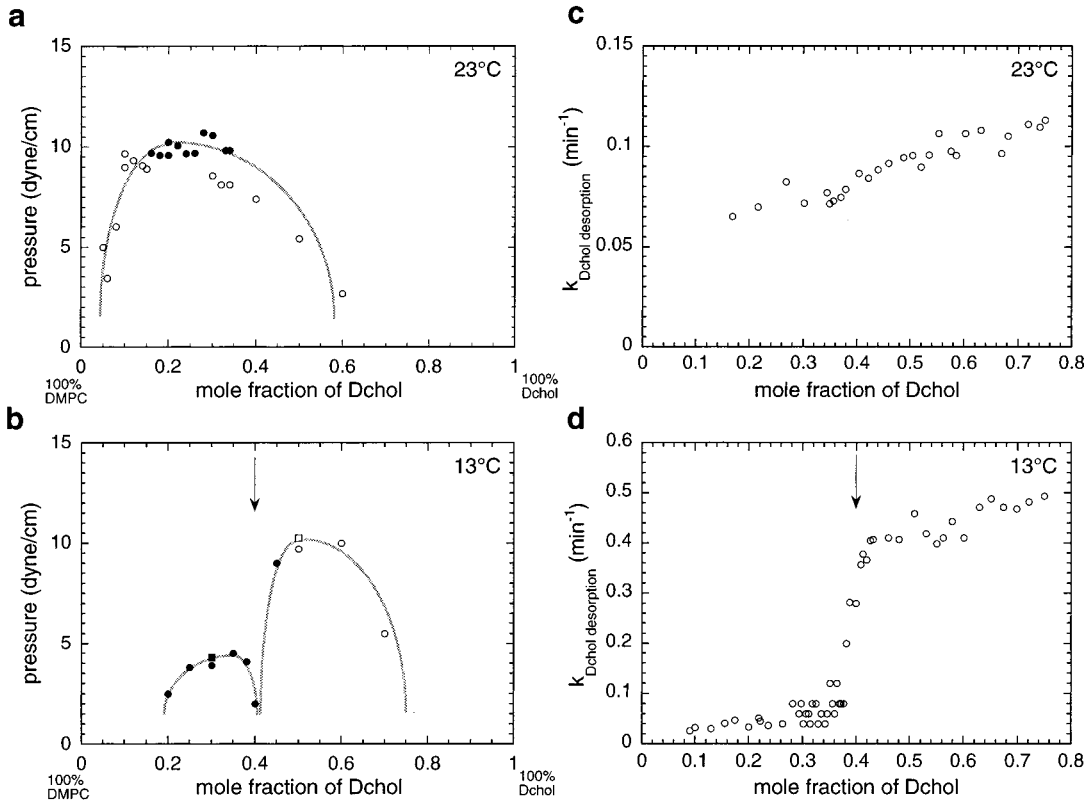

Figure 2. Experimental phase diagrams and desorption rates. Panels a and b show liquid−liquid miscibility phase diagrams for monolayer mixtures of DMPC and Dchol at 23 °C[14] and 13 °C. Data points (circles refer to Dchol, squares refer to cholesterol) represent transition pressures where two liquid phases transform into a single homogeneous phase. The stripe superstructure phases, which are diagnostic of proximity to a critical point,[33] were observed at the transitions marked by filled circles and squares and were not observed at those marked by open circles and squares. Panels c and d show rate constants (min^{-1}) for Dchol release from single-phase, homogeneous monolayer membranes to β-CD. These rate constants are calculated from the area decrease data such as those in Figure 3a and b and the molecular area data from Figure 3c and d. Area measurements were carried out at a surface pressure of 20 dyn/cm. The arrows in panels b and d are at $x_0 = 0.4$, which corresponds to the putative stoichiometry $q/(p + q) = 0.4$.

$q/(p + q)$ is obtained from the location of the cusp in the phase diagrams, the π_{ij}'s are close to the critical pressures of the respective two-phase miscibility peaks in the phase diagrams, and $\Delta\hat{A}$ is determined from molecular area measurements. The values of these experiment-based parameters in this study are $q = 2$, $p = 3$, $\Delta\hat{A} = -65$ Å^2, $\pi_{CP} = 12$ mN/m, $\pi_{CX} = 12$ mN/m, and $\pi_{PX} = 6$ mN/m, where X refers to the complex $C_{nq}P_{np}$. The values for other parameters such as n, ΔH_P, $\hat{K}^0_{eq}$, and a'_{ij} are chosen so as to produce calculated phase diagrams and chemical activities that mimic the temperature sensitivity of the data as well as possible. The best-fit parameters used are $n = 2$, $a'_{CX} = a'_{PX} = a'_{CP} = -1/6$ m/mN, $\hat{K}^0_{eq} = 0.3$, and $\Delta H_P = -9$ kcal/mol of P.

Results

Figure 2a and b show phase diagrams obtained for DMPC−Dchol mixtures in monolayers at room temperature (23 °C) and at a lower temperature (13 °C.). The phase diagram of 2a has been reported previously.[14] In 2b, phase-transition pressures at two of the compositions are given for cholesterol (squares) as well as Dchol (circles). At the higher temperature, the phase diagram shows no evidence of complex formation, whereas the phase diagram obtained at the lower temperature displays the characteristics of complex formation that have been discussed in detail earlier.[6,8] These conclusions are based not only on the shapes of the binodal curves but also on domain shapes and sizes previously described as characteristic of mixtures that do and do not exhibit complex formation.[6,8]

Figure 2c and d give the rate constants for Dchol desorption from the monolayer at 23 and 13 °C, respectively, the desorbed Dchol being captured by β-CD. As discussed earlier,[7] there are theoretical reasons to believe that this desorption rate is proportional to the chemical activity of cholesterol. At the lower temperature, the cusp in the phase diagram and the jump in the desorption rate occur at the putative stoichiometry of the condensed complex. This stoichiometry corresponds to $p = 3$ and $q = 2$.

The Dchol desorption rate constants are deduced from the rate of decrease of the membrane area at constant pressure in the presence of β-CD, which traps Dchol lost from the membrane. Illustrative data are given in Figure 3a and b for 23 and 13 °C, respectively. The analysis of data of this type in terms of a rate constant for Dchol loss requires knowledge of the average molecular area as a function of membrane composition. Measurements of such average areas are given in Figure 3c and d for 23 and 13 °C, respectively. Both data sets correspond to a surface pressure of 20 dyn/cm where only one liquid phase is present. Abrupt changes in slope in either or both data sets can contribute to the observed abrupt changes in calculated specific rate constants. In studies of other mixtures, sharp breaks in area versus time measurements were seen.[7] Also, sometimes quite pronounced cusps in area versus composition plots are seen. The calculated desorption rates represent a convolution of both sets of data. In the present work, the DMPC−Dchol complexes formed at 13 °C are evidently weaker, as judged by weak breaks in the area versus time curves (Figure 3b) and only a small cusp in the average molecular area versus

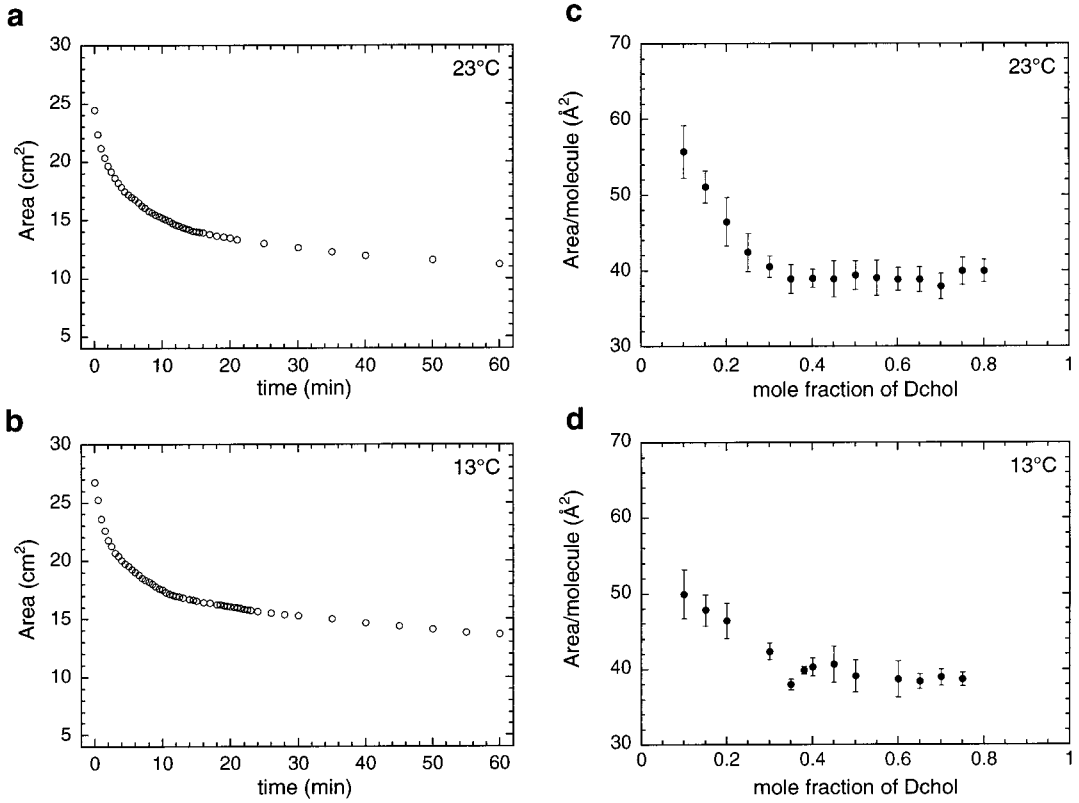

Figure 3. Desorption (monolayer area vs time) and average molecular areas. Panels a and b show sample plots of the area of a DMPC/Dchol monolayer kept at a constant surface pressure of 20 dyn/cm during Dchol desorption to a subphase of 1 mM β-CD at 23 and 13 °C, respectively. The monolayers contained 75 mol % Dchol initially. Panels c and d show average molecular area measurements for DMPC/Dchol mixtures at temperatures of 23 and 13 °C, respectively, at a surface pressure of 20 dyn/cm. Error bars represent deviations during three independent measurements.

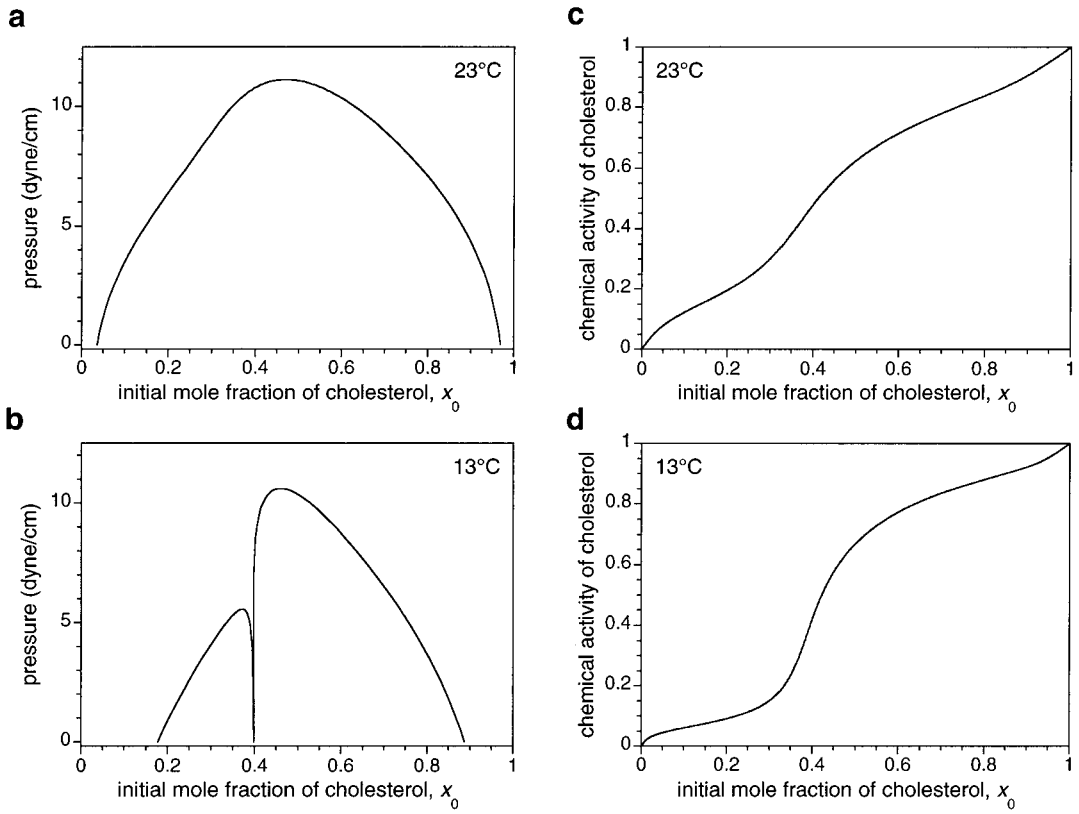

Figure 4. Theoretical phase diagrams and chemical activities. Panels a and b show calculated pressure (π)−composition (x_0) phase diagrams for reactive mixtures containing cholesterol and phospholipid at 23 and 13 °C, respectively. Compositions of coexisting phases were found by the method of double-tangent construction using the free energy of eq 2 and the parameters listed in the text. Panels c and d show calculated chemical activity−composition curves (x_0) for reactive mixtures of cholesterol and phospholipid at a pressure of 20 mN/m and at temperatures of 23 and 13 °C, respectively for the same parameters. The normalized equilibrium constant $\hat{K}_{eq}^{0}$ is 0.3, and the cooperativity n is 2.

composition curves (Figure 3d). Nonetheless, the calculated desorption rates show a pronounced jump at the stoichiometric composition at the lower temperature, as expected for complex formation. Repeated experiments resulted in slightly different (±8%) plateau values for the rate constants in the case of Figure 2d, but the sharp break always occurred at the same composition. In the case of Figure 2c, repeated experiments always resulted in similar curves with no jump.

Figure 4a and b give illustrative calculated pressure−composition phase diagrams for a reactive mixture of cholesterol and phospholipid at 23 and 13 °C, respectively, for the parameters listed above. In a search of parameter space, we have found that the magnitudes of the parameters that are consistent with the observed results are constrained. The immiscibility parameters used are similar to those used previously to describe liquid−liquid immiscibilities in other Dchol−phospholipid mixtures.[15] In Figure 4, the values of the normalized equilibrium constant $\hat{K}_{eq}^{0}$ and the cooperativity n are smaller than those employed previously for other mixtures,[15,16] which is consistent with the idea that the complexes studied here are weaker. Substantially larger values for these parameters have been used for DMPC−cholesterol mixtures in bilayers in connection with simulations of their calorimetry.[17] No effort was made to mimic the marked asymmetry of the binodal curve in Figure 2a, which requires higher-order terms in the free energy, as discussed elsewhere.[18] For the parameters used here, the equilibrium constant K_{eq} in eq 5 at a pressure of 20 dyn/cm changes from 50 at 23 °C ($\hat{K}_{eq}$= 7) to 1600 at 13 °C ($\hat{K}_{eq}$= 40). Figure 4c and d give calculated cholesterol chemical activity curves as a function of the initial cholesterol concentration, x_0, for a surface pressure of 20 dyn/cm at 23 and 13 °C, respectively. The activities calculated in Figure 4c and d are to be compared with the rate data in Figure 2c and d.

Figure 5 details the transition of the pressure−composition phase diagram from that of Figure 4b to 4a. On increasing the temperature, a triple-point line is first apparent at 14 °C (Figure 5a). This triple-point line moves up in pressure and disappears between 16 °C (Figure 5c) and 17 °C (Figure 5d).

Figure 6a and b show the calculated complex concentrations (mole fraction) as a function of the initial mole fraction of cholesterol, x_0, in the sample. The pressures are just below (1 dyn/cm) and above (3 dyn/cm) the triple-point line (at 1.8 dyn/cm) in the phase diagram shown in Figure 5b for 15 °C. The solid and dotted lines show the effects of phase separations. The solid line shows the mole fraction of the complex averaged over the coexisting phases as described by the lever rule. The dotted line shows the mole fraction of the complex in a hypothetical homogeneous phase of composition x_0. Figure 6c and d show the normalized free energy, $G/(N_0k_BT)$, as a function of x_0 at a temperature and pressure corresponding to those in Figure 6a and b, respectively.

Figure 7 gives the calculated normalized extent of reaction γ_{eq}/γ_{max} at the stoichiometric composition as a function of temperature. Curve a uses the parameters employed in the present paper for a pressure of 20 dyn/cm. Curve b uses the same parameters as are used in curve a except that the immiscibility parameters a_{ij} are set equal to zero. Curve c is derived from parameters used to simulate the DMPC−cholesterol calorimetry for bilayers.[17] Curves a and c are to be compared in that they seek to mimic experimental data. The temperature at which the extent of reaction is changing most rapidly is used to define the thermal decomposition temperature. The decomposition temperature in bilayers is about 5 °C higher than that in monolayers. The thermal decomposition temperatures are indicated in Figure 7a−c by open circles. The comparison of curves a and b shows that in the model calculations the immiscibility parameters that are used tend to stabilize the complex in the absence of phase separation.

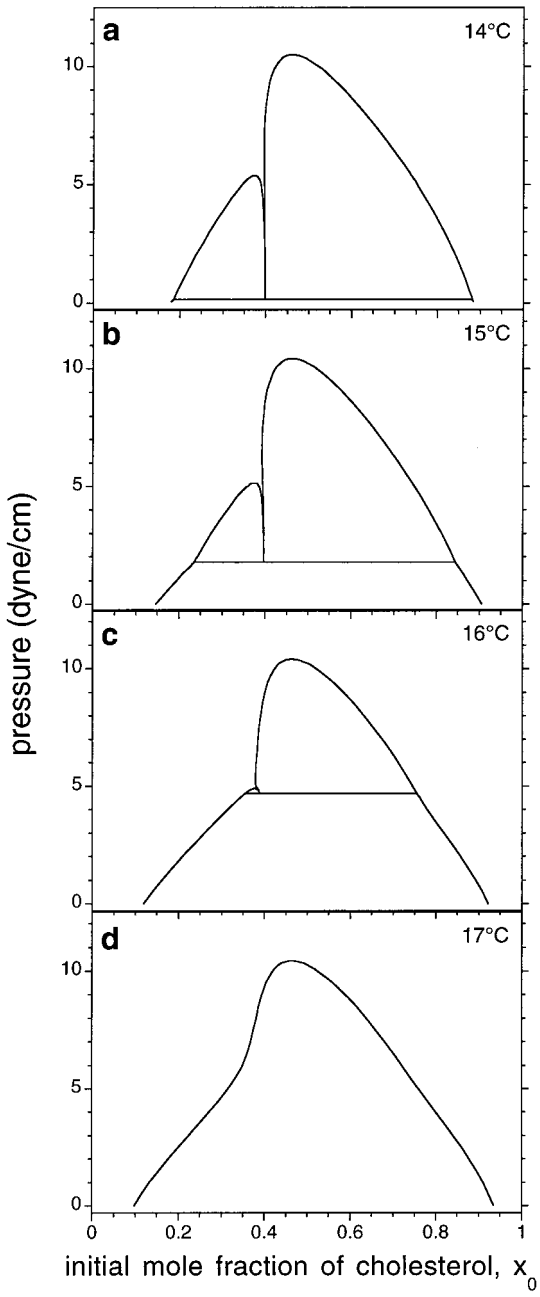

Figure 5. Theoretical phase diagrams at intermediate temperatures. Panels a−d show calculated pressure (π)−composition (x_0) phase diagrams for reactive mixtures containing cholesterol and phospholipid at temperatures between 13 and 23 °C for the parameters listed in the text.

Discussion

The experiments described here show clear evidence for the formation of complexes between Dchol and DMPC at 13 °C but not at 23 °C, which implies that the heat of reaction to form the complexes is substantial and exothermic. Our best estimate is that this heat of reaction is $\Delta H_P = -9$ kcal/mol of phospholipid (~14 k_BT in magnitude). This heat of reaction provides the best modeling of the observed thermal change in both the experimental phase diagrams and in the chemical activity curves. For the immiscibility parameters used, lower

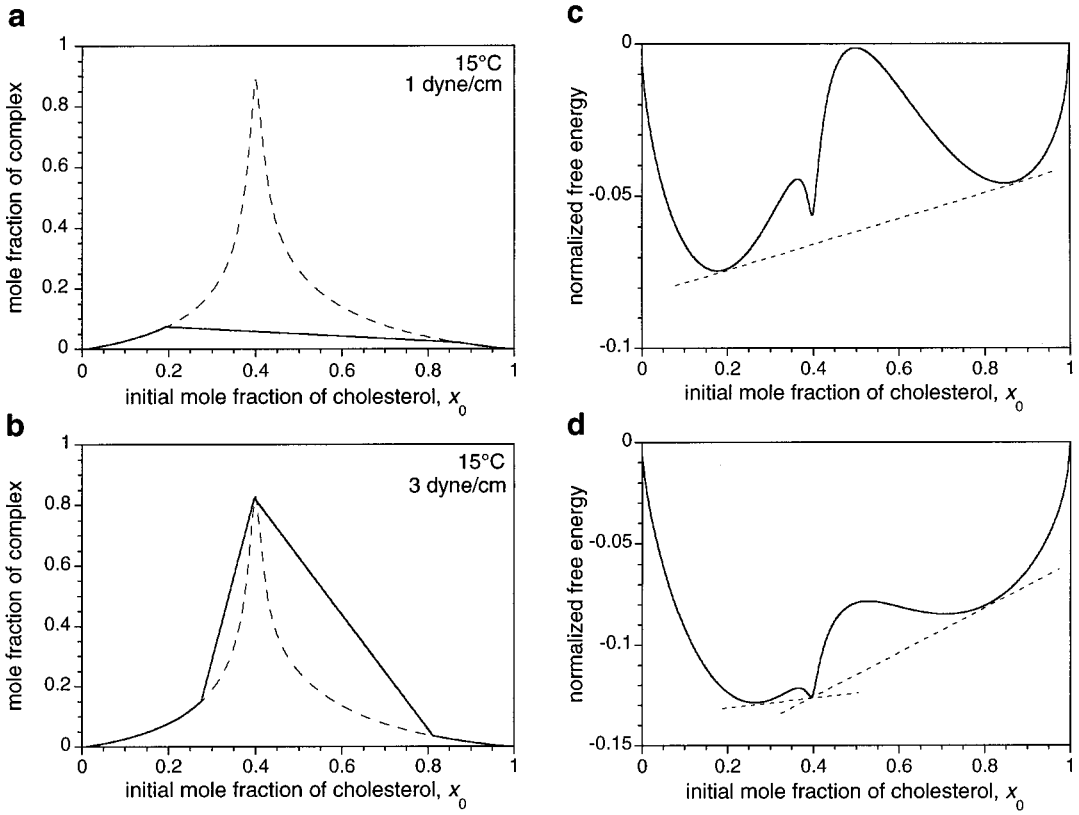

Figure 6. Effect of immiscibilities on complex formation. Panels a and b show calculated complex concentrations as a function of the initial mole fraction of cholesterol, (x_0), in the sample for a reactive mixture of cholesterol and phospholipid at a temperature of 15 °C and at pressures of 1 and 3 dyn/cm respectively (see Figure 5b). The solid lines show complex concentrations (mole fractions) in the presence of phase separations. The dotted lines show complex mole fractions in a hypothetical homogeneous phase of composition x_0. Panels c and d show normalized free-energy plots (G/N_0k_BT) as a function of the initial mole fraction of cholesterol, (x_0), in the sample for the same conditions as those in panels a and b, respectively. Lipid compositions between the tangent points exhibit two-phase coexistence (dotted lines).

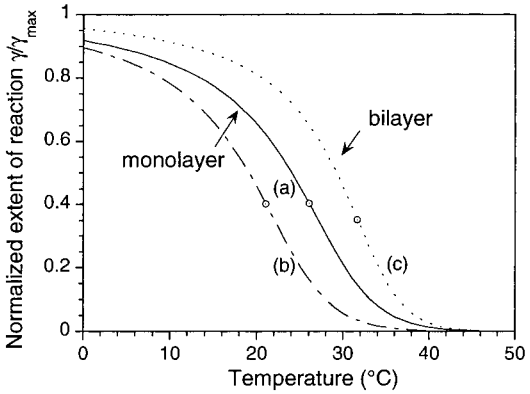

Figure 7. Temperature dependence of the normalized extent of reaction. Curves a−c show calculated normalized extents of reaction γ_{eq}/γ_{max} at the stoichiometric composition as a function of temperature. Curve a is calculated using the parameters listed in the text for a pressure of 20 dyn/cm. Curve b is also calculated for 20 dyn/cm but with immiscibilites a_{ij} set to zero. Curve c is taken from an unpublished calculation by T. Anderson using the parameters in ref 16.

values of $|\Delta H_P|$ could not be used for any modeling of the experimental data. As discussed below, this exothermic heat can be compared with the scanning calorimetry of binary mixtures of DMPC and cholesterol.

Early experiments on the scanning calorimetry of DMPC−cholesterol mixtures revealed the presence of broad heat absorptions.[4,19] These heat absorptions were attributed to cholesterol−phospholipid complexes having specific compositions. The scanning calorimetry experiments have been extensively refined in subsequent work.[20] In recent work, we have interpreted this broad heat absorption in terms of the thermal dissociation of condensed complexes.[17] The bilayer mixtures of DMPC and cholesterol show a broad heat absorption at 32 °C. The integrated heat absorption is 6 kcal/mol of phospholipid; thus, the heat of reaction to form complexes in monolayers is of the same order of magnitude as this putative heat of reaction in bilayers. In the simulation of the bilayer mixtures, the phospholipid/cholesterol stoichiometry was taken to be 3:1 with a cooperativity of $n = 12$. The decomposition temperature was about 32 °C, at which temperature the normalized extent of reaction is 35% (see Figure 7c). In the monolayer mixtures, the extent of reaction depends on the temperature and immiscibilities, as illustrated in Figure 7, and also on the pressure (not shown). The decomposition temperature of the complexes in monolayers is seen to be some 5 °C lower than that for the complexes in bilayers.

This work predicts that at appropriate temperatures and pressures monolayer mixtures of Dchol and DMPC will show a discontinuous transition at the triple-point lines seen in Figure 5a−c. On passing through the triple-point line, either by a change of pressure or temperature, there is a discontinuous change in the composition of the coexisting lipid domains as well as a discontinuous change in the concentration (mole fraction) of the complex. This behavior is shown for a change of pressure by the solid curves in Figure 6a and b. By way of contrast, the dotted curves in Figure 6a and b show calculated complex concentrations in a hypothetical homogeneous phase of composition x_0 for which there is little change on changing the pressure.

The thermodynamic model we have used is admittedly approximate, and the fit to the data is only semiquantitative.

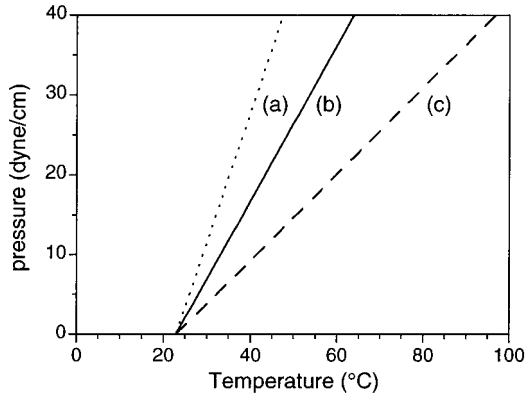

Figure 8. Compensating temperatures and pressures that leave K_{eq} invariant. Lines a−c describe conditions where the ratio K_{eq}/K_{eq}^0 in eq 5 is constant (equal to 1) for various values of ΔH_P. The other parameters are the same as those listed in the text. The values of ΔH_P in lines a−c are −15, −9, and −5 kcal/mol of phospholipid, respectively.

However, the prediction of a sharp, first-order phase transition is relatively unambiguous and should provide another strong experimental test of the model. In attempting to test this prediction experimentally, one should note the calculated free energy versus composition curves given in Figure 6c and d. It will be seen that there is the possibility of hysteresis (metastability) in the vicinity of the triple-point line, close to the stoichiometric composition, can be seen. That is, points within the phase diagrams with compositions near the stoichiometric composition can be outside the spinodal curves so that hysteresis of the first-order transition is possible at these compositions.

In earlier work, it was argued that the broad heat absorption in bilayer mixtures of cholesterol and DMPC is due to the thermal dissociation of condensed complexes composed of these two lipids.[17] The present work demonstrates that in monolayers these complexes are indeed thermally unstable. Therefore, thermal instability of condensed complexes must play a significant role in affecting the physical properties of the bilayers. These properties include liquid−liquid-phase separations in mixtures containing phospholipids and cholesterol.[21−27] These thermal effects on liquid−liquid immiscibility are distinct from those described in other theoretical models of these mixtures in bilayer mixtures.[28−32] Calculated temperature−composition phase diagrams are given in the Appendix.

Appendix

Temperature−Composition Phase Diagrams. It is useful to convert the theoretical models of pressure−composition phase diagrams to temperature−composition phase diagrams. This conversion provides a means of comparing phase diagrams of monolayers and bilayers because bilayer data will involve temperature−composition diagrams. The relation is somewhat complicated by the interplay of two distinct effects. According to the model parameters, increasing (monolayer) pressure and increasing (monolayer and bilayer) temperature suppress liquid−liquid immiscibilities. On the other hand, increasing monolayer pressure increases complex stability, whereas increasing temperature decreases complex stability in both monolayers and bilayers. The two effects can compensate for one another. For example, when K_{eq}/K_{eq}^0 is set equal to some constant, say 1, eq 5 reduces to

$$\pi = \left(\frac{T - T^0}{T^0}\right)\frac{\Delta\hat{H}}{\Delta\hat{A}} \qquad (9)$$

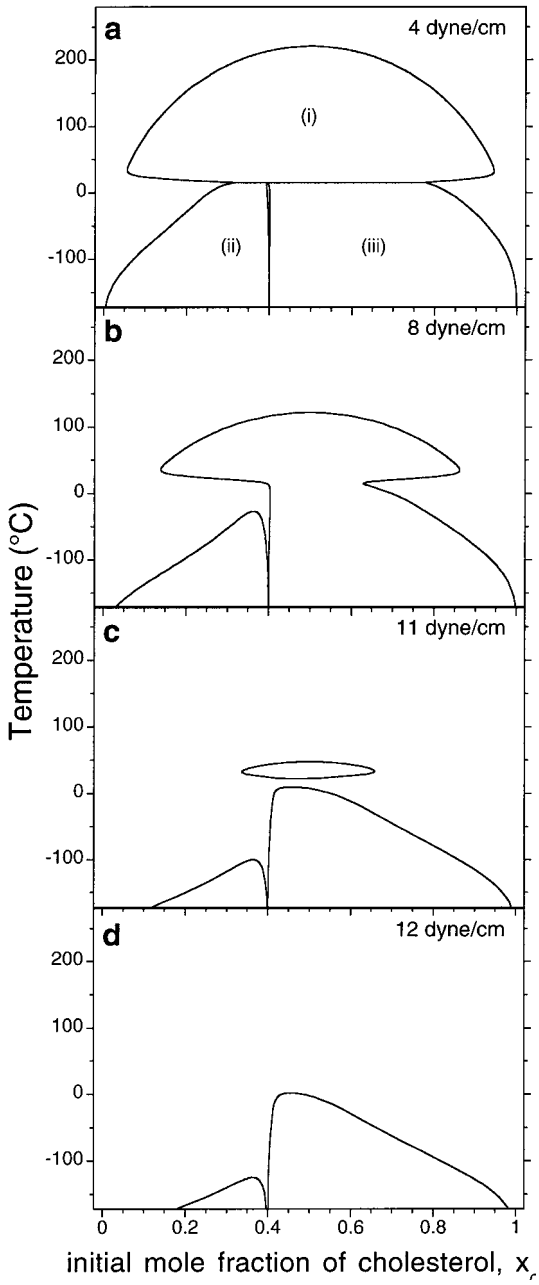

Figure 9. Temperature−composition phase diagrams in panels a−d show calculated temperature−composition phase diagrams for pressures of 4, 8, 11, and 12 dyn/cm, respectively. The parameters employed are the same as those used in Figure 4. In panel a, the labels (i), (ii), and (iii) refer to three distinct classes of two-phase coexistence regions (see text).

This compensating interplay between the temperature and pressure dependencies of K_{eq} is illustrated in Figure 8 where eq 9 is plotted for various values of ΔH_P (see Figure legend). This simple relationship is not useful quantitatively in the presence of immiscibility interactions, as illustrated already in Figures 6a and b and 7. Figure 7 shows that even in the absence of liquid−liquid phase separation the immiscibility parameters can have a substantial effect on complex concentrations.

Figure 9 gives a number of temperature−composition phase diagrams calculated with the same parameters used to calculate the phase diagrams in Figures 4 and 5. These diagrams do not include the solid phospholipid phase (important in bilayers[17]) because this phase is not seen in the monolayer experiments involving DMPC. In Figure 9a−d, one can easily identify three classes of two-phase coexistence regions. They are predomi-

nantly (i) (phospholipid-rich liquid)−(cholesterol-rich liquid), (ii) (phospholipid-rich liquid)−(complex-rich liquid), and (iii) (complex- rich liquid)−(cholesterol-rich liquid). In Figure 9a at $\pi = 4$ dyn/cm, there is a triple-point line at 15.6 °C. As discussed above, there is a discontinuous change in the composition of the coexisting lipid domains and in the concentration of the complex on passing through the triple-point line. The two-phase regions of type (ii) and (iii) below 15.6 °C are separated by a narrow one-phase region predominantly composed of the complex. The two-phase region above 15.6 °C is of type (i). The triple-point line disappears at a pressure of 8 dyn/cm in Figure 9b, when the type (ii) two-phase coexistence region separates. The type (i) two-phase coexistence region gets smaller with increasing pressure (Figure 9b and c) before completely disappearing at $\pi = 12$ dyn/cm in Figure 9d. The two-phase coexistence regions of types (ii) and (iii) persist at the higher pressures (Figure 9d) but only at low temperatures. For the parameters used, there is no liquid−liquid immiscibility of any kind above 0 °C for the high pressure of 20 dyn/cm. Monolayers at such high pressures are thought to be the closest mimic of the corresponding bilayers.

Acknowledgment. We are indebted to Tom Anderson, Sarah Keller, and Thomas Fischer for helpful discussions. We thank Ka Yee Lee for the use of her laboratory in an early phase of this work. This research was supported by the NIH.

References and Notes

(1) Leathes, J. B. *Lancet* **1925**, *208*, 853−856.
(2) Finean, J. B. *Experientia* **1953**, *9*, 17−19.
(3) Finean, J. B. *Chem. Phys. Lipids* **1990**, *54*, 147−156.
(4) Feingold, L. *Cholesterol in Membrane Models*; CRC Press: Ann Arbor, 1993.
(5) Radhakrishnan, A.; McConnell, H. M. *J. Am. Chem. Soc.* **1999**, *121*, 486−487.
(6) Radhakrishnan, A.; McConnell, H. M. *Biophys. J.* **1999**, *77*, 1507−1517.
(7) Radhakrishnan, A.; McConnell, H. M. *Biochemistry* **2000**, *39*, 8119−8124.
(8) Keller, S. L.; Radhakrishnan, A.; McConnell, H. M. *J. Phys. Chem. B* **2000**, *104*, 7522−7527.
(9) Subramaniam, S.; McConnell, H. M. *J. Phys. Chem.* **1987**, *91*, 1715−1718.
(10) Hirshfeld, C. L.; Seul, M. *J. Phys. (Paris)* **1990**, *51*, 1537−1552.
(11) Benvegnu, D. J.; McConnell, H. M. *J. Phys. Chem.* **1993**, *97*, 6686−6691.
(12) Corrales, L. R.; Wheeler, J. C. *J. Chem. Phys.* **1989**, *91*, 7097−7112.
(13) Talanquer, V. *J. Chem. Phys.* **1992**, *96*, 5408−5421.
(14) Hagen, J. P.; McConnell, H. M. *Biochim. Biophys. Acta* **1996**, *1280*, 169−172.
(15) Radhakrishnan, A.; McConnell, H. M. *Proc. Natl. Acad. Sci. U.S.A.* **2000**, *97*, 1073−1078.
(16) Radhakrishnan, A.; Anderson, T. G.; McConnell, H. M. *Proc. Natl. Acad. Sci. U.S.A.* **2000**, *97*, 12422−12427.
(17) Anderson, T. G.; McConnell, H. M. *Biophys. J.* **2001**, *81*, 2774−2785.
(18) Lee, K. Y. C.; McConnell, H. M. *Biophys. J.* **1995**, *68*, 1740−1751.
(19) Hinz, H.; Sturtevant, J. M. *J. Biol. Chem.* **1972**, *247*, 3697−3700.
(20) McMullen, T. P. W.; Lewis, R. N. A. H.; McElhaney, R. N. *Biochemistry* **1993**, *32*, 516−522.
(21) Gliss, C.; Clausen-Schaumann, H.; Gunther, R.; Odenbach, S.; Randl, O.; Bayerl, T. M. *Biophys. J* **1998**, *74*, 2443−2450.
(22) Bagatolli, L. A.; Gratton, E. *Biophys. J* **2000**, *78*, 290−305.
(23) Dietrich, C.; Bagatolli, L. A.; Volovyk, Z. N.; Thompson, N. L.; Levi, M.; Jacobson, K.; Gratton, E. *Biophys. J* **2001**, *80*, 1417−1428.
(24) Rinia, H. A.; Snel, M. M. E.; van der Eerden, J. P. J. M.; de Kruijff, B. *FEBS Lett.* **2001**, *501*, 92−96.
(25) Samsonov, A. V.; Mihalyov, I.; Cohen, F. S. *Biophys. J* **2001**, *81*, 1486-1500.
(26) Yuan, C.; Johnston, L. J. *Biophys. J* **2001**, *81*, 1059−1069.
(27) Dietrich, C.; Volovyk, Z. N.; Levi, M.; Thompson, N. L.; Jacobson, K. *Proc. Natl. Acad. Sci. U.S.A.* **2001**, *98*, 10642−10647.
(28) Ipsen, J. H.; Karlstrom, G.; Mouritsen, O. G.; Wennerstrom, H.; Zuckermann, M. J. *Biochim. Biophys. Acta* **1987**, *905*, 162−172.
(29) Ipsen, J. H.; Mouritsen, O. G.; Zuckermann, M. J. *Biophys. J.* **1989**, *56*, 661−667.
(30) Nielsen, M.; Miao, L.; Ipsen, J. H.; Zuckermann, M. J.; Mouritsen, O. G. *Phys. Rev. E* **1999**, *59*, 5790−5803.
(31) Sugar, I. P.; Tang, D.; Chong, P. L. *J. Phys. Chem.* **1994**, *98*, 7201−7210.
(32) Somerharju, P.; Virtanen, J. A.; Cheng, K. H. *Biochim. Biophys. Acta* **1999**, *1440*, 32−48.
(33) Keller, S. L.; McConnell, H. M. *Phys. Rev. Lett.* **1999**, *82*, 1602−1605.